第7回地震時保有耐力法に基づく橋梁等構造の
耐震設計に関するシンポジウム講演論文集（2004年1月）

ENHANCEMENT OF SEIEMIC PERFORMANCE OF RC STRUCTURES BY CONTROLLING BOND OF REINFORCEMENT

Govinda Raj Pandey[1], Hiroshi Mutsuyoshi[2]

[1]Graduate Student, Structural Material Laboratory, Saitama University （〒338-0811 Sengokusho 201, Shirakuwa 24-4, Sakura-ku, Saitama-shi, Saitama）
[2]Professor, Dept. of Civil and Environmental Engineering, Saitama University（〒338-8570 Shimo-Okubo, Sakura-ku, Saitama-shi, Saitama ）

1. Introduction

Predicting the flexural response of RC members is relatively well understood and well established while shear behavior remains as a complex phenomenon. Despite numerous research on shear behavior, which have been intensively carried out following the collapse of warehouse at Wilkins Air Force Depot at Ohio in 1955[1),2)], to construct a structure avoiding undesirable shear collapse still poses a great challenge. Shear failure is catastrophic in nature and is responsible for the loss of structural integrity and eventual collapse of the structure, which is potentially dangerous both in terms of safety and economy. The recent severe earthquakes such as Northridge Earthquake (1994) and Hyogoken-Nanbu Earthquake (1995), also demonstrated that the bridges without shear failure survived collapse in spite of the severe flexural damage[3),4)]. Unlike buildings, bridge structures possess low degree of indeterminacy and shear failure of one pier may lead to the total collapse of the whole structure. Particularly, short piers are more susceptible to shear failure due to the higher shear to moment ratio.

The investigation on the bridges damaged by earthquake shows that shear failure mainly occurs due to the inadequacy of web reinforcements apart from the deficient reinforcement detailings[5)]. As conventional codes do not take size effect into account, it leads the design of large RC members in unsafe side. In case of reversed loadings, such as earthquake, structures may undergo shear failure even after yielding of longitudinal bar[6)]. It is therefore understood from the investigation that the quantity of shear reinforcement obtained from the conventional design codes, which are basically empirical equations developed from the numerous experimental investigations with monotonic loading on RC beams, may lead the unsafe design.

The lessons learnt from the disasters further expedited intensive study and wide range modification have been incorporated in design codes in order to prevent undesirable shear failure. Apart from the modifications in the detailing conditions most of the codes have increased the amount of web reinforcement as the primary way to avoid shear failure.

Large amount of shear reinforcements however has given rise to another set of problems. The members designed with the recent codes require a large amount of shear reinforcements. Large number of reinforcements however makes the detailing of the member complicated and the congestion leads to the difficulty in placing concrete. It therefore becomes counterproductive both in terms of constructability and economy. This underscores the need to investigate some alternative ways of shear capacity improvement without the heavy reliance on web reinforcements alone.

Elimination of the bond between longitudinal bar and concrete leads to major change in stress distribution inside the concrete[7)]. With no flexural cracks in unbonded shear span, it is apparent that the concrete body mainly remains under diagonal compression with straight thrust line resembling an arch mechanism. Thus, this stress condition makes the whole shear span to be free of cracks. This condition is effective in preventing diagonal shear crack, which can eventually enhance the shear performance of columns[8)-12)].

The main purpose of this study is to investigate the possible enhancement of seismic performance of RC bridge piers such as shear strength and ductility by controlling bond of longitudinal reinforcement. The aim is also to conduct rigorous analysis on seismic response behavior of RC columns with unbonded reinforcement and compare them with that of the columns with ordinary deformed bars.

2. Experimental Program

In order to investigate the influence of unbonding reinforcement on seismic behavior of RC columns, six specimens were tested under reversed cyclic loading.

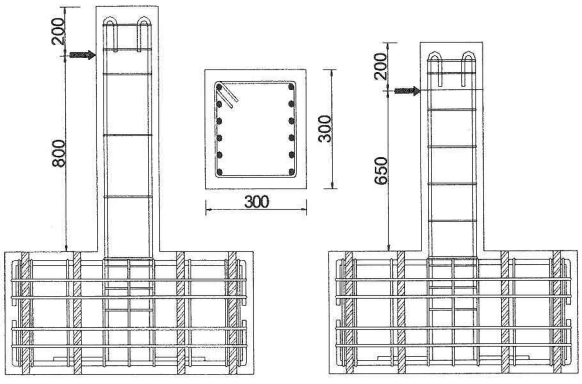

A-Series B-Series

Fig-1 Details of column specimens

(1) Specimen Details

Specimens were divided into two series depending on shear-span-to-depth (a/d) ratio. **Fig-1** shows the geometry and reinforcement details of the test specimen. Every specimen consisted of column part cast monolithically with footing part. Cross-section of all the specimens were 300 x 300 mm while the height if the columns were 1000 mm and 850 mm for specimens of A-Series and B-Series respectively. Shear capacity of concrete, was evaluated by using Okamura-Higai as shown in equation **(1)**.

$$V_c = 0.2 f_c'^{1/3} (100 p_w)^{1/3} (\tfrac{1000}{d})^{1/4} (0.75 + 1.4 \tfrac{d}{a}) b_w d \quad (1)$$

where,
f_c' = compressive strength of concrete
p_w = ratio of tensile longitudinal steel area to area of web concrete
d = effective depth
a = shear span
b_w = web width of member

Okamura-Higai equation was used because it incorporates the effect of a/d ratio. Design shear strength to flexural strength ratio of 0.8 was employed in the experiment. Identical longitudinal reinforcement details with 12 bars of 16 mm in diameter were incorporated in all the test specimens. Deformed bars with the diameter of 6 mm were used as lateral reinforcement. **Table-1** shows the details of the test specimens.

Table-1 Details of the column specimen

Sp. No.	a/d	Bond condition	Longitud -inal bars A_s	Lateral ties Size and spacing(mm)
A-1	3.0	Deformed bars	12-D16	D6@250
A-2		Unbonded bars	12-D16	D6@250
A-3		Round bars	12-φ16	D6@250
B-1	2.5	Deformed bars	12-D16	D6@150
B-2		Unbonded bars	12-D16	D6@150
B-3		Round bars	12-φ16	D6@150

(2) Material Properties

Ready-mix, normal weight concrete with an average slump of 150 mm was used. Compressive strength test on concrete cylinders and tensile strength test on steel samples were performed to determine the actual material properties of the concrete and reinforcing steel. **Table-2** presents the compressive strength of concrete on the day of cyclic loading test and the yield strength of the various types of steel used in the specimen.

Table-2 Material properties of the column specimen

Sp. No.	Concrete f_c', MPa	Longitudinal bars f_y, MPa	Lateral ties f_{wy}, MPa
A-1	32.54	380.18	396.60
A-2	33.69	380.18	396.60
A-3	34.12	324.06	396.60
B-1	28.76	380.18	396.60
B-2	30.47	380.18	396.60
B-3	31.14	324.06	396.60

(3) Method of Controlling Bond

From perfect bond to the perfect unbond, a total number of three bond conditions were used to investigate the influence of bond. **Fig-2** shows the methods used in bond control. In the specimens with perfect bond normal deformed bars were used as longitudinal reinforcement. Poor bond condition was achieved by replacing deformed bars with round bars. The surface of the round bar in shear span was smoothened by using sand paper which was then followed by the application of grease before placing the concrete.

(a) Poor Bond (b) Perfect Unbond

Fig-2 Method of controlling bond

Complete unbonding of longitudinal bar was achieved by the use of spiral sheath. Before casting the specimen, the desired length of longitudinal bar was inserted into the sheath. The location of the sheath was properly fixed and the both the end of the sheath were made water tight by applying silicon gel.

(4) Experimental Setup and Instrumentation

Fig-3 shows the loading setup. The specimen was fixed on the floor with prestressing rods. Reversed cyclic lateral load was applied at the designated loading point of the column by using an actuator. A constant axial load of 90 kN was applied throughout the experiment in order to maintain the compressive stress of 1 MPa. Axial loading jack was designed to move freely with applied lateral displacement.

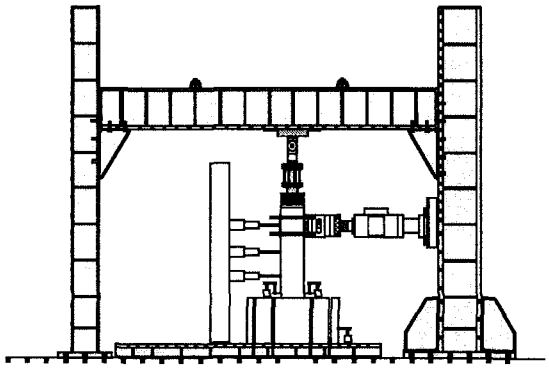

Fig-3 Experimental setup

Horizontal displacements at three different locations in the column, crack width at the column-footing joint and possible displacement and rotation of the specimen were measured by displacement transducers. Strains in several locations of both longitudinal bars and lateral reinforcement were measured by using strain gages which were already fixed at the desired location before placing concrete.

(5) Reverse Cyclic Loading Test

All the specimens were subjected to reverse cyclic quasistatic loading with the loading sequence shown in **Fig-4**. Each displacement amplitude was prolonged for a set of three cycles. The first set of cycles was essentially within the elastic range and with the increase in the number of cycles the specimen entered to the inelastic range. In the first set of cycles, the specimen was subjected to the displacement amplitude of H/200, where H is the height of the lateral loading point from the column base. Displacement amplitude was then increased with an increment of H/200 until the specimen failed. The specimen was considered to have failed when the load carrying capacity was reduced to the 80% of its maximum recorded load.

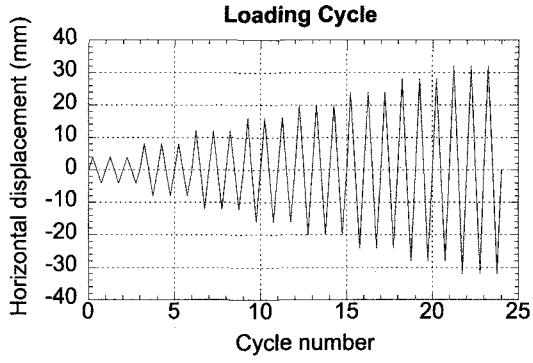

Fig-4 Loading sequence

3. Results and Discussion

(1) Load-Displacement Curve

Load-displacement curves obtained from the experiment for both A-Series and B-Series are shown in **Fig-5**. Specimen A-1 failed in shear before yielding of the longitudinal bars. Specimen A-2 with unbonded longitudinal bars completely avoided shear failure and eventually failed due to crushing and spalling of concrete followed by yielding of longitudinal bars. Specimen A-3 with rounds bars applied with grease coating showed better performance with significant improvement in ductility. Unlike A-1, Specimen B-1 failed in shear after the longitudinal bars yielded. With the change in the bond condition, similar to A-Series, B-Series also showed improvement in ductility and complete change in the failure mechanism from shear to flexure.

Pinching effect was clearly visible in the load displacement curves. This effect was attributed to the closure of diagonal shear crack with the load reversal in the case of Specimens A-1 and B-1. On the other hand, pinching in unbonded specimens was due to the closure of large flexural crack at column-footing joint.

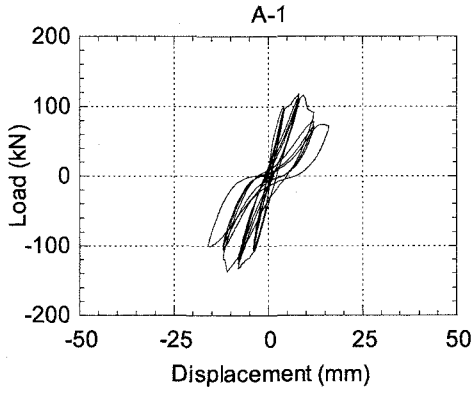

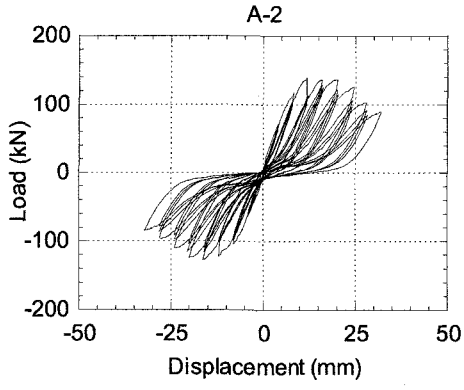

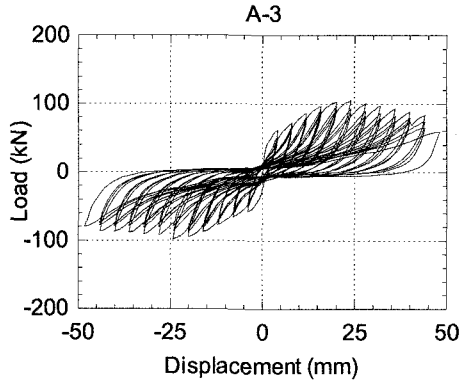

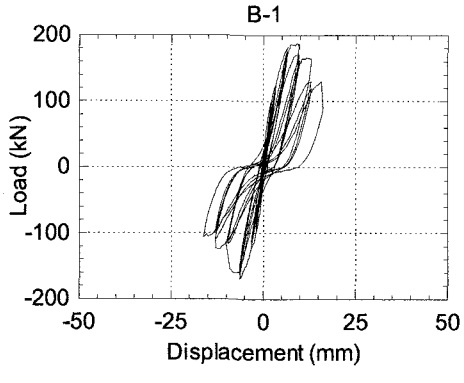

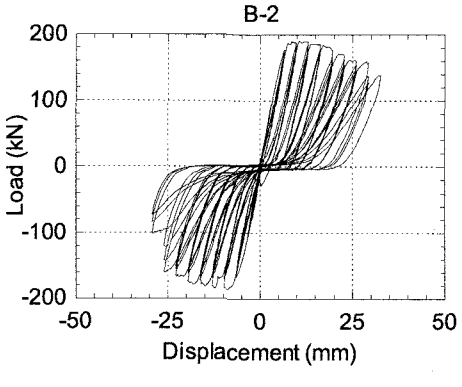

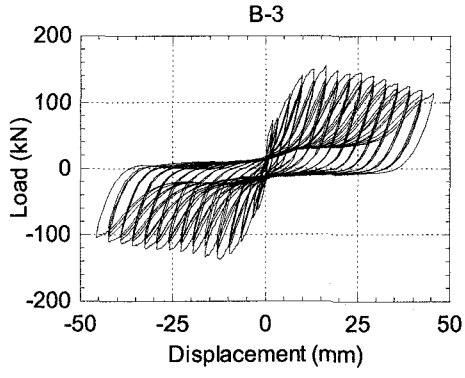

Fig- 5 Load displacement curves of all tested specimens

(2) Failure Pattern

Fig-6 shows the crack pattern of all the specimens at failure. In the case of specimens A-1 and B-1, flexural cracks occurred at the several locations on the specimen right from the first cycle. As the number of cycles increased, the crack furthered and then developed to diagonal shear crack. The final failure took place with the wide opening of diagonal crack resulted from the yielding of shear reinforcement. Load-displacement curve clearly shows a typical shear behavior.

In case of specimens A-2 and B-2, the crack started from the column-footing joint first. With further loading the crack at the bottom increased and propagated upwards. No single crack was formed at the sides of the specimen. The final failure was due to the crushing of concrete followed by yielding of the longitudinal bars.

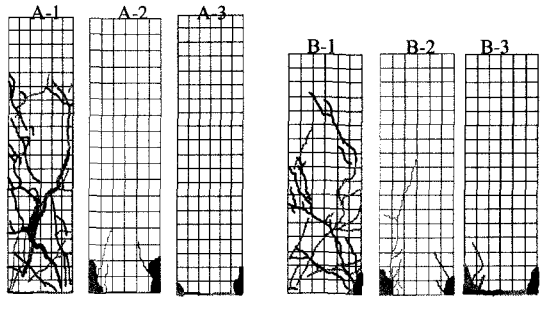

Fig-6 Crack pattern of specimens at failure

Specimens A-3 and B-3 also performed in a manner similar to specimen A-2 and B-2. It showed a better performance as the damage was concentrated only at the column-footing joint. The final failure was due to the crushing of concrete followed by yielding of the longitudinal bars.

(3) Envelope Curves

Comparison of load-displacement envelope curve in both the series is shown in **Fig-7**. The envelope curves in

A-Series show that, by unbonding, the load carrying capacity of the specimen was increased due to the complete change in failure mechanism. It was also observed that there was a slight reduction of stiffness due to unbonding but remarkable increase in ductility. The best performing specimen was the one with round bar applied with grease. It showed flexural failure with more ductile behavior. The load carrying capacity of the specimen with round bars, however, seemed to reduce but that was attributed to the lower tensile strength of round bar than that of deformed bars.

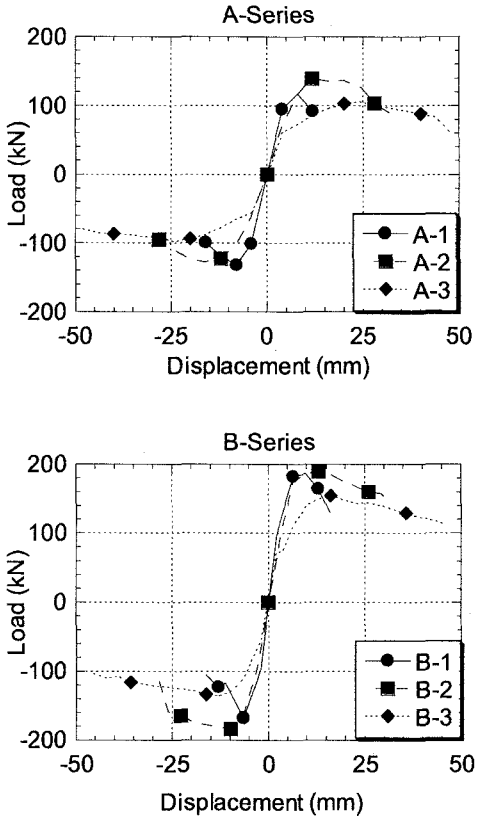

Fig-7 Load displacement envelope curves

B-Series also demonstrated the similar phenomena. Remarkable improvement in ductility was found in the unbonded specimen with a very little reduction in stiffness and delayed yielding. The performance further improved by replacing the longitudinal bars with round bars applied with grease.

(4) Strain Distribution in Longitudinal Bar

Fig-8 presents the comparison of strain in the longitudinal bars of specimens B-1 and B-2 at three different locations. The first one was 10 mm above the column-footing joint whereas the second and the third one being at 170 mm and 250 mm above the column-footing joint respectively. Specimen B-1 showed a large difference in the magnitude of strain at those locations. Strain was found to be primarily concentrated near the column footing joint. In the case of specimen B-2, however, the difference was found to be minimal. The strain, instead of concentrating on the critical region, averaged on the whole unbonded length.

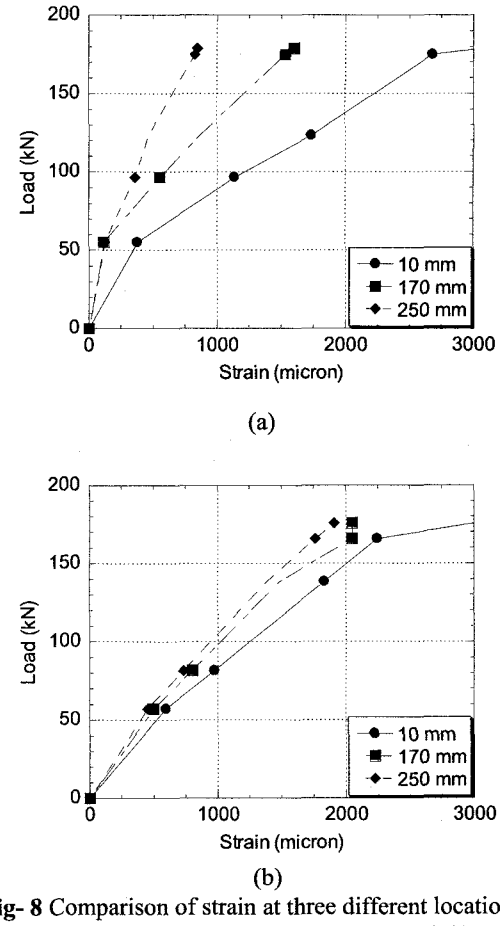

Fig- 8 Comparison of strain at three different locations of longitudinal bars for specimen (a) B-1 and (b) B-2

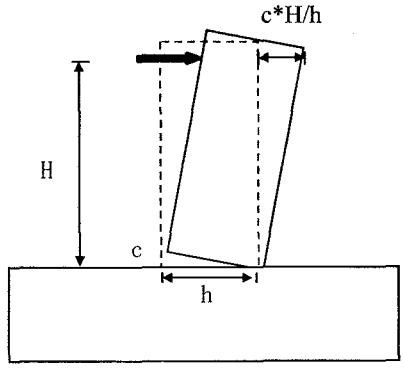

Fig-9 Displacement due to rigid body rotation

(5) Comparison of Displacement due to Crack at Base

In order to study the mechanism of the unbonded reinforced concrete column, displacement at the loading point was calculated from the crack width measured at column-footing joint assuming the specimen acts as a rigid body. **Fig-9** schematically shows the relation between crack width c and displacement at the loading point. The calculated displacement was then compared with the measured value.

Fig-10 (a) shows a clear disagreement between calculated and actual displacement. As specimen B-1 failed in shear, majority of the displacement was contributed by flexural and shear deformation. **Fig-10** (b), however, shows that the calculated displacement agreed well with the experimental results in specimen B-2.

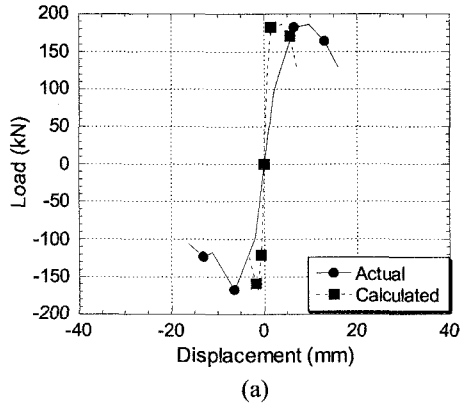

(a)

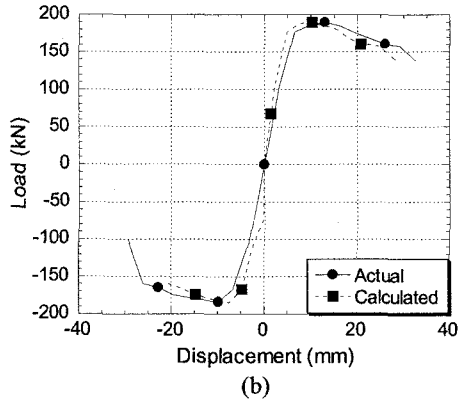

(b)

Fig-10 Comparison of displacement calculated by rigid body analogy with actual value

4. Seismic Response Analysis

Though the impressive improvement in shear resistance and ductility has been evident as a result of unbonding longitudinal bar, the major setback of this method is the low area of energy absorption and high residual deformation. To study the behavior of unbonded columns against earthquake loading, seismic response analysis has been carried out.

(1) Restoring Force Model

Among various restoring force models proposed by several researchers, Takeda's Model is the most commonly accepted one. In this study, a stiffness degrading model with a bilinear skeleton has been used to model the ordinary reinforced concrete column[13),14)]. Schematic diagram of the model is presented in **Fig-11**.

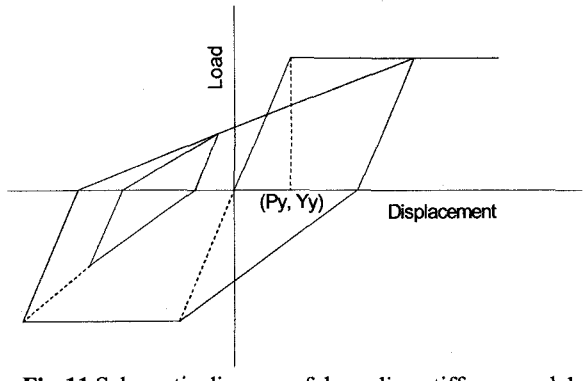

Fig-11 Schematic diagram of degrading stiffness model

The model however is not able to model the unbonded columns as sharp pinching occurs in the hysterisis loop due to wide crack at the column footing joint. A large discrepancy can be observed when the model is compared with the experimental results as shown in **Fig-12**.

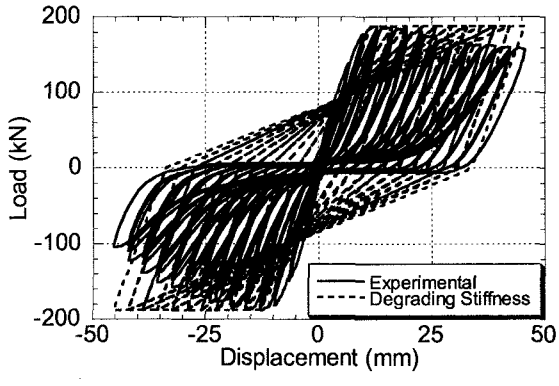

Fig-12 Comparison of degrading stiffness model with experiment

A new model has been proposed with the similar bilinear skeleton but the straight loading curve has been replaced by power equation as explained in equation **(2)**

$$P = A(Y - Y_{start})^Z + P_{start} \quad \textbf{(2a)}$$

$$A = (P_{go} - P_{start})/(Y_{go} - Y_{start})^Z \quad \textbf{(2b)}$$

$$Z = 2.2\ln((Y_{go} - Y_{start})/Y_y) + 1 \quad \textbf{(2c)}$$

Where, (P,Y) it the coordinate of the loading curve between (Pstart,Ystart) and (Pgo,Ygo).

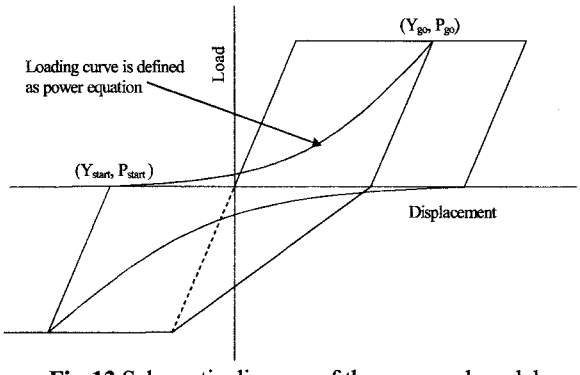

Fig-13 Schematic diagram of the proposed model

The schematic diagram of the proposed model is shown in **Fig-13**. This model is very much versatile in nature. If Z is defined to be unity, it yields the ordinary degrading stiffness model. **Fig-14** shows that the model has good agreement with the experimental results.

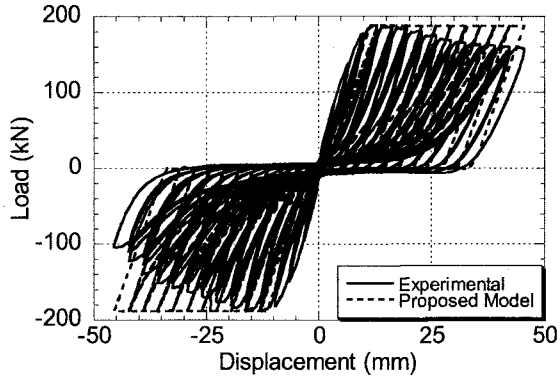

Fig-14 Comparison of proposed model with experiment

(2) Nonlinear Response Analysis

Two different earthquake waves were used in the analysis, namely, Hyogoken-Nanbu Earthquake (1995) and El Centro Earthquake (1940). Acceleration history of both the earthquakes is presented **in Fig-15**.

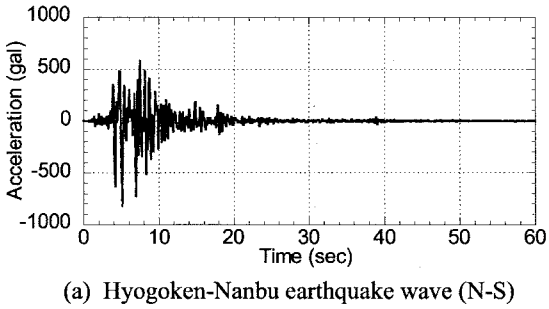

(a) Hyogoken-Nanbu earthquake wave (N-S)

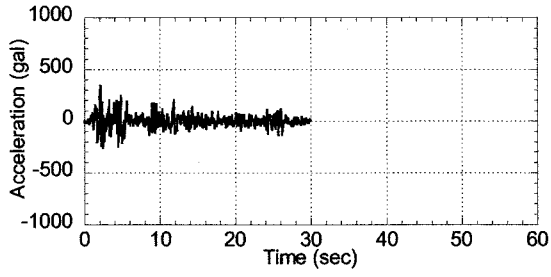

(b) El Centro earthquake wave (N-S)

Fig-15 Earthquake waves used in the analysis

Response analysis with each earthquake was carried out for two different yield ratios. Yield ratio is defined as the ratio of yield strength of the column to the gravity load. **Fig-16** summarizes the results in terms of ductility spectrum. Ductility is defined as the ratio of maximum displacement to the yield displacement.

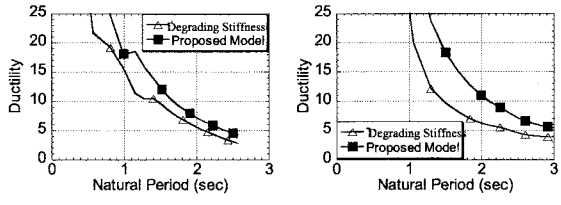

(a) Yielding Ratio = 0.6 (b) Yielding Ratio = 0.35

Fig-16 Ductility Spectrum of Hyogoken-Nanbu Earthquake

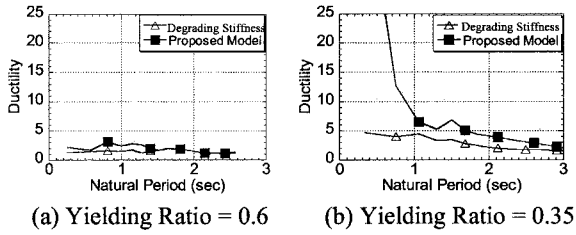

(a) Yielding Ratio = 0.6 (b) Yielding Ratio = 0.35

Fig-17 Ductility spectrum of El Centro earthquake

It can therefore be clearly observed that the unbonded columns yield larger displacement response as compared to the ordinary RC column. The difference becomes much prominent when the frequency of the earthquake becomes closer to the natural frequency of the column. This difference is attributed to the low area of energy absorption and hence the low damping of the unbonded columns.

4. Conclusion

Reversed cyclic loading test was carried out on six RC columns with various bond conditions of longitudinal reinforcement. Nonlinear seismic response analysis was also carried out to compare the behavior of unbonded columns with the ordinary one. Based on this study following conclusions can be drawn:

1. Unbonding of longitudinal bar can completely change failure mode at the ultimate state from shear to flexure and it remarkably increases the ductility.
2. Due to unbonding, strain in longitudinal bar gets averaged throughout the unbonded length. This results yielding of reinforcing bars to delay. Longer length of unbond further retards yielding.
3. Though both unbonding longitudinal bar and replacing deformed bars with greased round bars improve seismic behavior, the later technique yields better performance which is attributed to the poor bond of longitudinal bar embedded into the footing.
4. Behavior of unbonded specimen is close to a rigid body with damage being concentrated at column-footing joint alone. Upper part of the column does not show significant change in stress due to lateral load.
5. Unbonding of longitudinal bar however results in the lower area of energy absorption and larger residual deformation which is responsible for larger seismic response especially when the frequency of the earthquake becomes closer to the natural frequency of the column.

References

1) ACI-ASCE Committee 445 on Shear and Torsion: Recent approaches to shear design of structural concrete, *Journal of Structural Engineering*, Vol. 124, No. 12, pp. 1375-1417, 1998.
2) Hsu, T. T. C.: Unified approach to shear analysis and design, *Cement and Concrete Composites*, Vol. 20, pp. 419-435, 1998.
3) Kawashima K.: Seismic design and retrofit of bridges, *Proceeding of 12th World Congress on Earthquake Engineering*, 2228, 2000.
4) Okamura, H.: Japanese seismic design codes prior to Hyogoken-Nanbu earthquake, Cement and Concrete Composites, Vol. 19, pp. 185-192, 1997.
5) Sezen, H. et al.: Performance of reinforced concrete buildings during the August 17, 1999 Kocaeli, Turkey earthquake, and seismic design and construction practice in Turkey, *Engineering Structures*, 25, pp.103-114, 2003.
6) An, Z., Maekawa, K.: Shear resistance and ductility of RC columns after yield of main reinforcement, *Journal of Materials, Concrete Structures, Pavements*, JSCE No. 585/V-38, February 1998, pp.233-247,1998.
7) Kani, G. N. J.: The riddle of shear failure and its solution, *ACI Journal*, Vol. 61, No. 4, pp. 441-467, 1964.
8) Ranasinghe, K., et al.: Effect of bond on shear behavior of RC and PC beams: experiments and FEM analysis, *Proceedings of JCI*, Vol.23, No. 3, pp.1057-1062, 2001.
9) Ranasinghe, K., et al.: Cyclic testing of reinforced concrete columns with unbonded reinforcement, *Proceedings of JCI*, Vol.24, No.2, pp.1141-1146, 2002.
10) Pandey, G. R. et al.: Mitigation of seismic damage of RC structures by controlling bond of reinforcement, *Proceedings of the Japan Concrete Institute*, Vol. 25, pp. 1441-1446, 2003.
11) Lees, J. M., Burgoyne, C. J.P: Experimental studies of influence of bond on flexural behavior of concrete beams pretensioned with aramid fiber reinforced plastics, *ACI Structural Journal*, Vol. 96, No. 3, pp.377-385, 1999.
12) Lees, J. M., Burgoyne, C. J.: Analysis of concrete beams with partially bonded composite reinforcement, *ACI Structural Journal*, Vol. 97, No. 2, pp.252-258, 2000.
13) Takeda, T. et al.: Reinforced concrete response to simulated earthquakes, *Journal of the Structural Division, proceedings of the American Society of Civil Engineers*, Vol. 96, No. ST12, pp. 2557-2573, 1970.
14) Clough, R. W., and Johnston, W. H.: Effect of stiffness degradation on earthquake ductility requirement, *Proceedings of Japan Earthquake Engineering Symposium*, Tokyo, Japan, pp. 195-198, 1966.